Theoretical Study on the Substitution Reactions of Silylenoid H_2SiLiF with CH_4, NH_3, H_2O, HF, SiH_4, PH_3, H_2S, and HCl

Ju Xie,[†,‡] Dacheng Feng,[*,†] and Shengyu Feng[†]

School of Chemistry and Chemical Engineering, Shandong University, Jinan 250100, People's Republic of China, and College of Chemistry and Chemical Engineering, Yangzhou University, Yangzhou 225002, People's Republic of China

Received: January 29, 2007; In Final Form: May 11, 2007

DFT calculations at the B3LYP/6-31G(d,p) level have been performed to explore the substitution reactions of silylenoid H_2SiLiF with XH_n hydrides, where XH_n = CH_4, NH_3, H_2O, HF, SiH_4, PH_3, H_2S, and HCl. We have identified a previously unreported reaction pathway on each reaction surface, $H_2SiLiF + XH_n \rightarrow H_3SiF + LiXH_{n-1}$, which involved the initial formation of an association complex via a five-membered cyclic transition state to form an intermediate followed by the substituted product H_3SiF with $LiXH_{n-1}$ dissociating. These theoretical calculations suggest that (i) there is a very clear trend toward lower activation barriers and more exothermic interactions on going from left to right along a given row in the periodic table, and (ii) for the second-row hydrides, the substitution reactions are more exothermic than for the first-row hydrides and the reaction barriers are lower. The solvent effects were considered by means of the polarized continuum model (PCM) using THF as a solvent. The presence of THF solvent disfavors slightly the substitution reaction. Compared to the previously reported insertions and H_2-elimination reactions of H_2SiLiF and XH_n, the substitution reactions should be most favorable.

1. Introduction

In recent years, considerable attention has been devoted to the investigation of silylenoid as an important silicon-reactive intermediate both in organosilicon chemistry and in organic synthesis.[1−3] Molecules with general formula R_2SiMX (R, substituents such as H, CH_3, Ph; M, usually alkali metals; X, usually halogens) are called silylenoid because their chemical behavior is similar to that of silylene R_2Si. However, the preparation of silylenoids, as a kind of very reactive species, is very difficult. Until 1995, Tamao[2c] reported the first experimental study of silylenoid chemistry, detected the existence of [(*tert*-butoxy)diphenylsilyl]lithium, $Ph_2SiLi(OBu\text{-}t)$, and investigated its chemical properties. In 2004, Lee[2g] reported the syntheses of stable halosilylenoids $(Tsi)X_2SiLi$ (Tsi = $C(SiMe_3)_3$; X = Br, Cl) at room temperature. In 2006, Molev[2j] reported the molecular structure of the first isolated fluorosilylenoid, $(R_3Si)_2SiFLi\cdot 3THF$ (R_3Si = *t*-Bu_2MeSi). Thus, a great breakthrough has been experimentally made in the research of silylenoids. The theoretical studies on silylenoids were lagging. In 1980, Clark[3a] studied theoretically the isomers of lithofluorosilylenoid H_2SiLiF by ab initio calculations for the first time. Since the 1990s, we have studied some silylenoids[3c−e] by quantum chemistry theory on their structures, stability, isomerization, insertion reactions, and addition reactions etc. Both experimental[2] and theoretical[3] results show that silylenoids have ambiphilic character, nucleophilicity and electrophilicity, and can take part in many reactions. Such reactions as insertion, addition, and polymerization were recognized as important and effective methods for preparation of the new silicon-bonded and heterocyclic silicon compounds. Therefore, further thorough investigations on silylenoids will be of important theoretical and practical value.

TABLE 1: The Relative Energies (E_r, kJ/mol) Including Vibrational ZPE (without Scale) of Various Structures in the Gas Phase at the B3LYP/6-31G(d,p) Level

	E_r		E_r
R + HF	0.0	**R** + HCl	0.0
		Clts	−35.4
Fim	−241.3	**Clim**	−258.4
H_3SiF + LiF	−170.0	**H_3SiF** + LiCl	−179.6
R + H_2O	0.0	**R** + H_2S	0.0
Opc	−111.4	**Spc**	−43.7
Ots	−104.8	**Sts**	−42.6
Oim	−148.1	**Sim**	−172.3
H_3SiF + **LiOH**	−82.4	**H_3SiF** + LiSH	−96.0
R + NH_3	0.0	**R** + PH_3	0.0
Npc	−106.5	**Ppc**	−42.8
Nts	−38.8	**Pts**	0.9
Nim	−66.5	**Pim**	−89.7
H_3SiF + $LiNH_2$	1.3	**H_3SiF** + $LiPH_2$	−16.0
R + CH_4	0.0	**R** + SiH_4	0.0
Cpc	−18.5	**Sipc**	−14.6
Cts	102.4	**Sits**	57.3
Cim	35.5	**Siim**	−46.3
H_3SiF + $LiCH_3$	102.0	**H_3SiF** + $LiSiH_3$	28.5

Most recently, we carried out a series of theoretical studies on the reaction potential energy surfaces of the three-membered ring[3a,d] silylenoid H_2SiLiF with XH_n hydrides, where XH_n = CH_4, NH_3, H_2O, HF, SiH_4, PH_3, H_2S, and HCl.[4] The results indicated that the insertion and H_2-elimination pathways of H_2SiLiF with XH_n all took place at the H_2Si moiety of H_2SiLiF.[5] However, the LUMO of H_2SiLiF consists mainly of orbitals of lithium atom.[3a,d] When the HOMO of XH_n approaches lithium

* Corresponding author. Fax: +86-0531-88564464. E-mail: fdc@sdu.edu.cn.
† Shandong University.
‡ Yangzhou University.

10.1021/jp070773a CCC: $37.00
Published on Web 08/09/2007

TABLE 2: NBO Analysis for R + H_2O Reaction in the Gas Phase

	Si	F	Li	H*	O	Si−Li	Si−H*	O−H*	LP_{Si}
R	0.328	−0.706	0.830			1.896			
H_2O				0.472	−0.944			1.999	
Opc	0.443	−0.711	0.894	0.430	−1.092			1.996	1.805
Ots	0.852	0.694	0.887	0.104	−1.180		1.948		
Oim	1.258	−0.653	0.842	−0.192	−1.329		1.976		
LiOH			0.872		−1.346				
H_3SiF	1.287	−0.613		−0.225			1.979		

of H_2SiLiF, what would be the reaction pathways? Which pathway is preferable? These arouse our interest to investigate the reaction potential energy surfaces of H_2SiLiF with XH_n again. Thus, the present calculations will provide the new reaction pathways, substitution reactions (1), on the $H_2SiLiF-XH_n$ reaction potential energy surfaces.

$$H_2SiLiF + H{-}XH_{n-1} \rightarrow H_3SiF + LiXH_{n-1} \qquad (1)$$

2. Computational Details

All calculations were performed using the Gaussian 03[6] suites of programs. The geometries of reactants, precursor complexes, transition states, and products were optimized at the B3LYP/6-31G(d,p) level.[7] The stationary points on the potential energy surface were characterized by calculations of vibrational frequencies at the same level. To verify that transition states actually connect to the expected reactants, intermediates, and products for each reaction, intrinsic reaction coordinate (IRC)[8] calculations were performed. The solvent effect is modeled using the self-consistent reaction field (SCRF) method with the Tomasi's polarized continuum model (PCM).[9] The PCM cavity is defined by using Bondi's atomic radii. Based on the B3LYP/6-31G(d,p) optimized geometries, natural bond orbital (NBO) analyses at the same level were then used.[10]

3. Results and Discussion

The calculation results show that the substitution reactions studied in this work follow the reaction pathway as shown in Scheme 1. It involves the initial formation of a precursor complex (**Xpc**), followed by a five-membered cyclic transition state (**Xts**) to form an intermediate (**Xim**) followed by the substituted product H_3SiF with $LiXH_{n-1}$ dissociating. The relative energies (relative to the corresponding reactants) are given in Table 1 (in the gas phase) and Table 3 (in THF solvent), respectively. The optimized geometries are given in Figures 1 and 3, in which the migratory hydrogen from X to Si, fluorine in HF, and silicon in SiH_4 are marked as H*, F*, and Si*, respectively.

3.1. Reactions of H_2SiLiF (R) with CH_4, NH_3, H_2O, and HF. To elucidate the substitution mechanism more distinctly, the **R** + H_2O reaction is discussed in detail, and then the general rules of **R** with XH_n are presented. Frontier molecular orbital analyses of **R** + H_2O reaction are shown in Figure 2, and NBO results are listed in Table 2.

Precursor Complexes. As shown in Figure 2, the LUMO of **R** consists mainly of orbital of the lithium atom. When the HOMO of H_2O approaches lithium, the precursor complex **Opc** forms (Figure 1). In **Opc**, Si, F, Li, O, and H* atoms are almost in the same plane. **Opc** is only slightly distorted from the reactant geometries. The O−H* bond is elongated slightly to 1.024 Å. However, the Li−O distance is shortened to 1.853 Å. The interaction between Li and O atoms makes the Si−Li bond weak, and one lone pair orbital (LP_{Si}: 1.805) locates on the Si atom. In fact, there also exists the weak attractive interaction between the HOMO of **R** and the LUMO of H_2O, and the Si−H* distance is 2.287 Å. These attractive interactions between **R** and H_2O make **Opc** being 111.4 kJ/mol more stable than the separated entities.

Transition States. As the reaction proceeds, the Si−Li bond is broken, and Li−O and Si−H* bonds nearly form. The reaction reaches the transition state **Ots**. **Ots** is a "loose" five-center pattern involving Si, F, Li, O, and H* atoms. In **Ots**, Li−O and Si−H* bonds are shortened to 1.752 and 1.734 Å, respectively, and the O−H* bond is stretched to 1.331 Å. Compared with those of **Opc**, the positive charge of Si atom increased obviously, and the charge of H* decreased obviously. The H* atom transferring from O atom to Si atom occurs from the **Opc** to **Ots** process. The energy of **Ots** is only 6.6 kJ/mol higher than that of **Opc**. It indicates that the reaction takes place easily at this calculational level.

TABLE 3: The Relative Energies (E_r, kJ/mol) Including Vibrational ZPE (without Scale) in THF Solvent at the B3LYP/6-31G(d,p) Level

	E_r		E_r
R + HF	0.0	**R** + HCl	0.0
		Clpc	−19.2
		Clts	−15.2
Fim	−235.1	**Clim**	−265.7
H_3SiF + LiF	−180.0	H_3SiF + LiCl	−206.7
R + H_2O	0.0	**R** + H_2S	0.0
Opc	−80.4	**Spc**	−32.9
Ots	−55.9	**Sts**	−25.6
Oim	−129.8	**Sim**	−174.9
H_3SiF + LiOH	−75.2	H_3SiF + LiSH	−116.6
R + NH_3	0.0	**R** + PH_3	0.0
Npc	−89.9	**Ppc**	−33.8
Nts	18.3	**Pts**	28.3
Nim	−43.8	**Pim**	−86.0
H_3SiF + $LiNH_2$	9.5	H_3SiF + $LiPH_2$	−28.6
R + CH_4	0.0	**R** + SiH_4	0.0
Cpc	−6.9	**Sipc**	−2.8
Cts	134.5	**Sits**	78.6
Cim	48.5	**Siim**	−45.8
H_3SiF + $LiCH_3$	99.2	H_3SiF + $LiSiH_3$	11.7

SCHEME 1

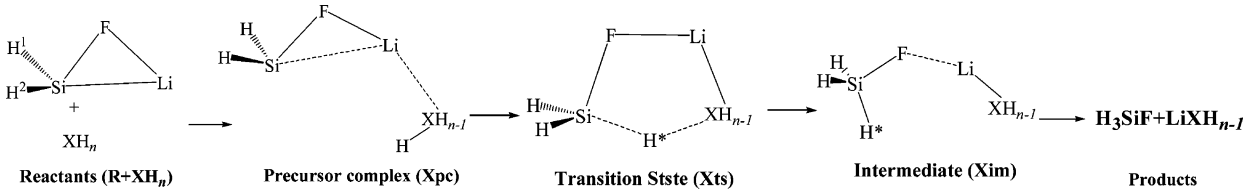

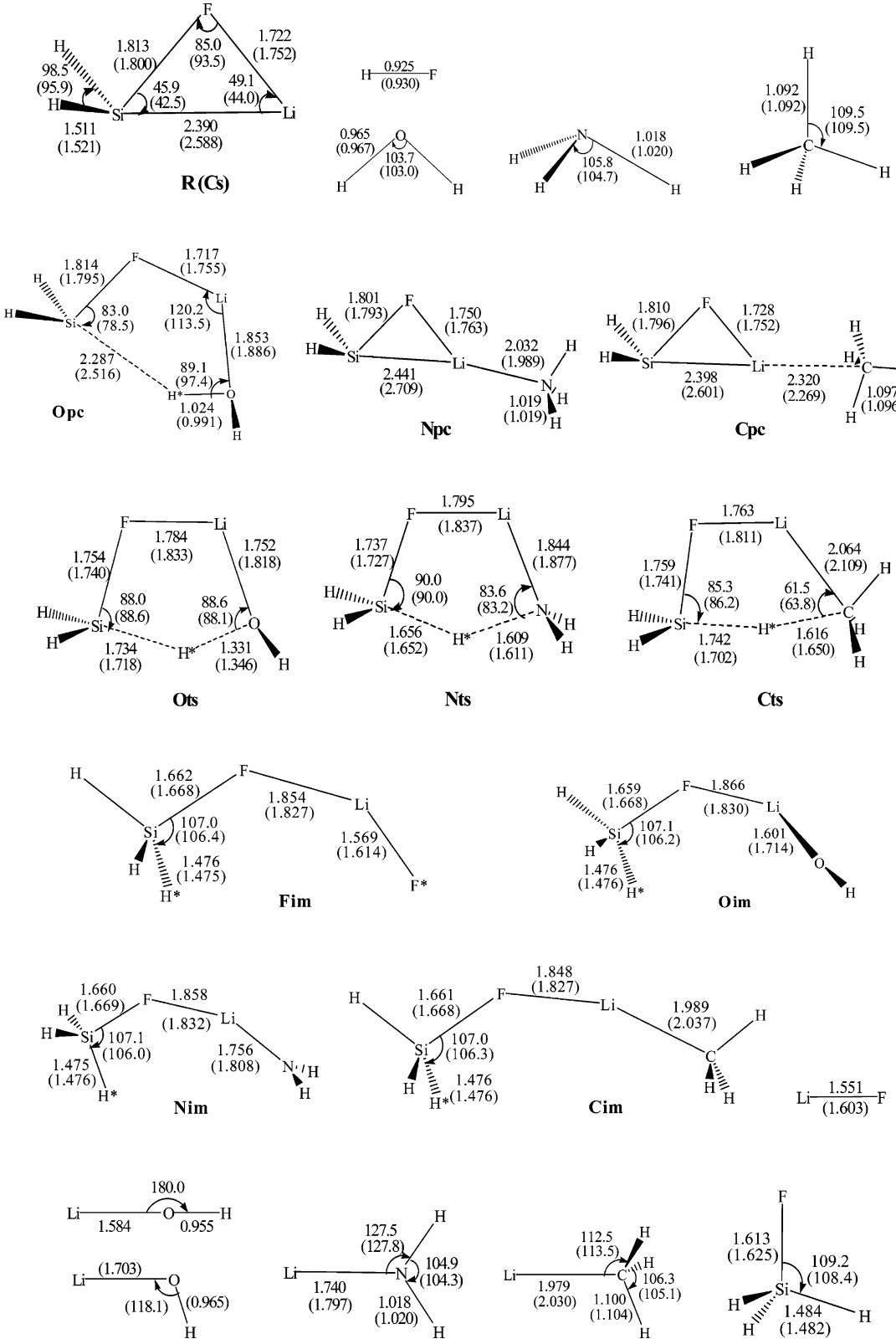

Figure 1. The B3LYP/6-31G(d,p) optimized geometries (bond lengths, Å; bond angles, deg) in the gas phase and THF (in parentheses) of H_2SiLiF (**R**) reactions with HF, H_2O, NH_3, and CH_4.

Substitution Intermediate. After getting over transition state **Ots**, the Si−H* and Li−O bonds formed with rupturing of the O−H* bond. The intermediate **Oim** forms. In **Oim**, Si atom adopts sp^3 hybridization bonding to three hydrogens and the fluorine. The F−Li bond is stretched by 0.082 Å. In fact, **Oim** is an electrostatic complex of substitution silane H_3SiF and LiOH via the interaction between negative F and positive Li atoms. Relative to the sum energies of **R** and H_2O, the energy of **Oim** is −148.1 kJ/mol.

Substitution Products. When the Li−F bond breaks off, H_3SiF and LiOH can be obtained. As a whole, Li atom of H_2SiLiF is replaced by H atom of H_2O. It can be found from the atoms in Table 2 that part of an electron on Si atom is transferred to H* and O atoms from the beginning of the reaction

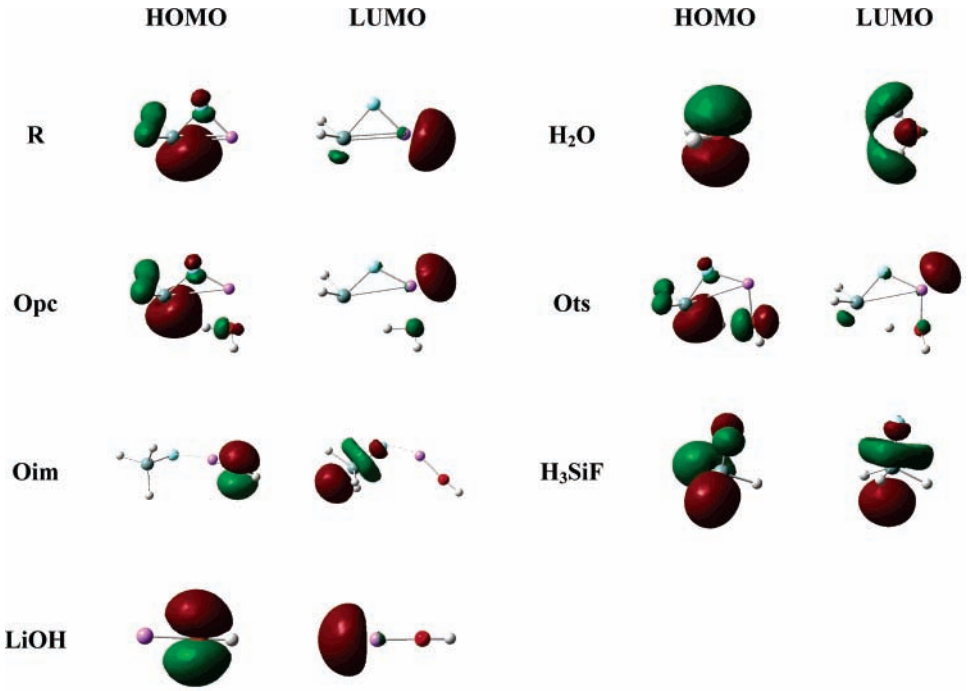

Figure 2. Frontier molecular orbital analyses of **R** + H_2O reaction in the gas phase.

to the transition state. That is, silylenoid H_2SiLiF moiety shows nucleophilic character. Therefore, the reaction proceeds via a nucleophilic substitution mechanism.

The reaction mechanisms of **R** with CH_4 and NH_3 are similar to that of **R** with H_2O. Because of the relative low electronegativity of C element as well as the steric effect of CH_4, the stability of precursor complex **Cpc** is very weak. The relative energy of **Cpc** is only −18.5 kJ/mol. NH_3 is a stronger ligand with a lone pair of electrons on N atom, which makes **Npc** stable. The relative energy of **Npc** is −106.5 kJ/mol. The transition states **Nts** and **Cts** appear to have similar structure to **Ots**. The relative energies of **Nts** and **Cts** are −38.8 and 102.4 kJ/mol, respectively, and the energies of **Nts** and **Cts** are 67.7 and 120.9 kJ/mol higher than those of **Npc** and **Cpc**, respectivey. As a result, the activation barrier for reactions of **R** with H_2O, NH_3, and CH_4 is in the order of H_2O < NH_3 < CH_4. It is reasonable to predict that the activation barrier for HF reaction is lower than that of H_2O reaction because of the highest electronegativity of F element. We do not find the precursor complex and transition state for HF reaction at the B3LYP/6-31G(d,p) level, and it is predicted that the reaction takes place much more easily. Four intermediates **Fim**, **Oim**, **Nim**, and **Cim** have similar structures. Their relative energies are −241.3, −148.1, −66.5, and 35.5 kJ/mol, respectively. The relative energies of products (H_3SiF and $LiXH_{n-1}$), reaction heats, is in the order of CH_4 (102.0 kJ/mol) > NH_3 (1.3 kJ/mol) > H_2O (−82.4 kJ/mol) > HF (−170.0 kJ/mol). In conclusion, the reactivity of **R** with the first-row hydrides increases in the order of CH_4 < NH_3 < H_2O < HF.

3.2. Reactions of H_2SiLiF (R) with SiH_4, PH_3, H_2S, and HCl. The calculational results indicate that the reaction processes of **R** with the second-row hydrides are similar to those of **R** with the first-row hydrides.

Precursor Complexes. As shown in Figure 3, the precursor complex structures of **R** with H_2S and PH_3, **Spc** and **Ppc**, are similar, in which weak electrostatic interactions exist between the lone pair electrons on S and P atoms with the positive Li atom, respectively. In the case of **Sipc**, there exists the weak static interaction between H atom in SiH_4 and Li atom in **R** because of the lower electronegativity of Si element than that of H element as well as the steric effect. The relative energies of the three precursor complexes are in the order of **Sipc** (−14.6 kJ/mol) > **Ppc** (−42.8 kJ/mol) > **Spc** (−43.7 kJ/mol). The precursor complex of **R** with HCl was not obtained at the B3LYP/6-31G(d,p) level.

Transition States. Four transition states, **Clts**, **Sts**, **Pts**, and **Sits**, are shown in Figure 3. In **Clts**, there exist the strong interaction between Li and Cl atom and the weak interaction between Si and H* atom. The Cl−H* bond is only 0.022 Å longer than that in the HCl molecule, and there is little variation in the structural parameters of the H_2SiLiF moiety relative to **R**. All these features indicate that the HCl reaction arrives at the transition state relatively early. The results of **Sts** for H_2S reaction are similar to those of the HCl reaction. In **Pts**, the P−H* distance is stretched by 0.286 Å, the Si−H* distance is shortened to 1.943 Å, and the Li−P bond is almost formed. In **Sits**, the Si*−H* distance is stretched by 0.307 Å, and the interaction between Si and H* atoms is obvious, whereas the interaction between Li and Si* atoms is still weak. The relative energies of the four transition states are in the order of **Sits** (57.3 kJ/mol) > **Pts** (0.9 kJ/mol) > **Clts** (−35.4 kJ/mol) > **Sts** (−42.6 kJ/mol).

Substitution Intermediate and Products. Four substitution intermediate structures, **Clim**, **Sim**, **Pim**, and **Siim**, are similar. Their relative energies are −258.4, −172.3, −89.7, and −46.3 kJ/mol, respectively. The relative energies of products (H_3SiF and $LiXH_{n-1}$) are in the order of SiH_4 (28.5 kJ/mol) > PH_3 (−16.0 kJ/mol) > H_2S (−96.0 kJ/mol) > HCl (−179.6 kJ/mol). In conclusion, the reactivity of **R** with the second-row hydrides increases in the order of SiH_4 < PH_3 < H_2S < HCl.

It can be found from the above discussion that the reactions of **R** with the first- and second-row hydrides proceed similarly via the nucleophilic substitution mechanism. The potential energy surface profiles along the reaction pathways of **R** + XH_n are shown in Figure 4. As shown in Figure 4, the substitution reaction trend of **R** with the first-row hydrides is the same as that of **R** with the second-row hydrides, and the reaction difficulty decreases on going from left to right along a given

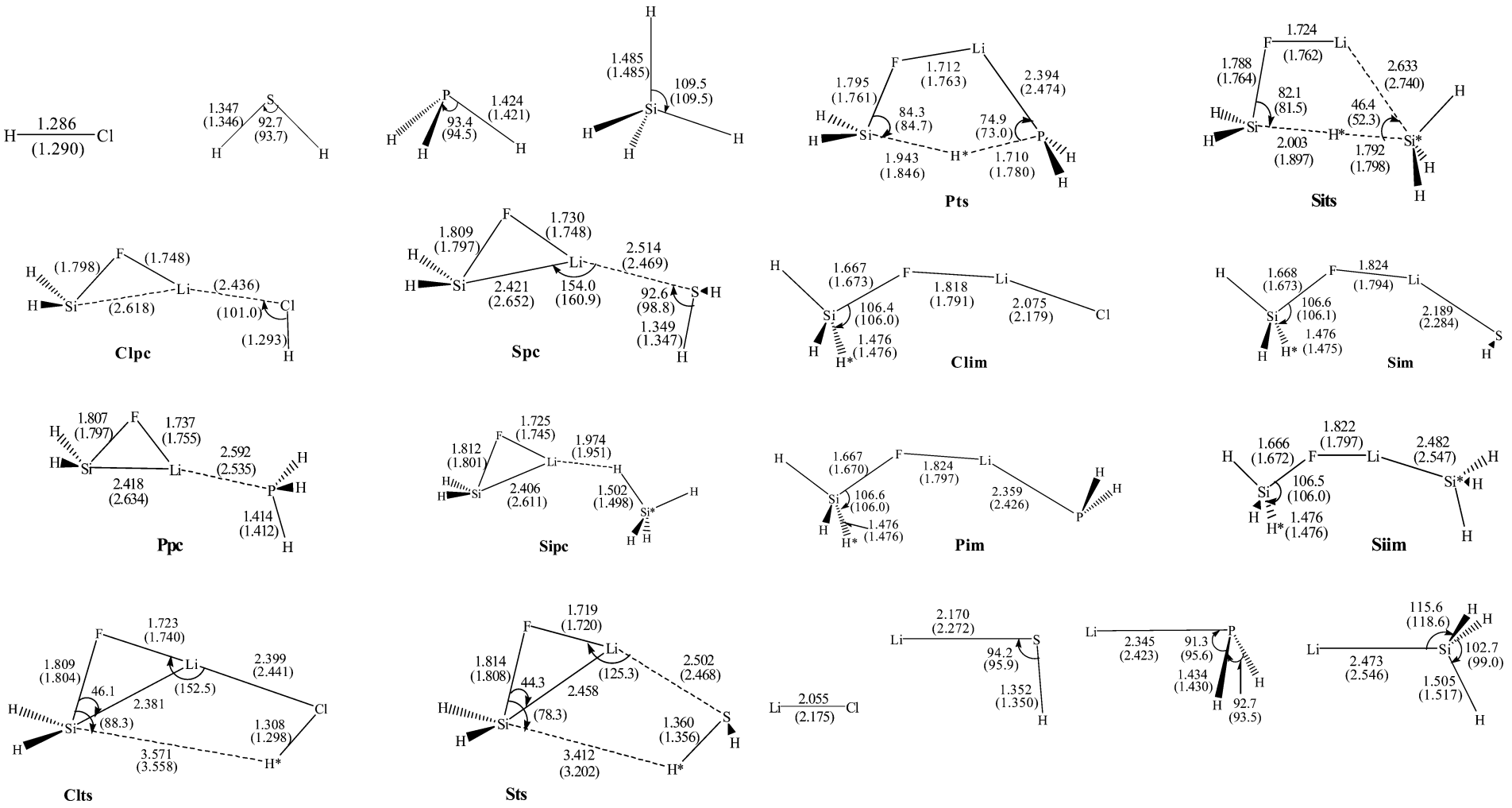

Figure 3. The B3LYP/6-31G(d,p) optimized geometries (bond lengths, Å; bond angles, deg) in the gas phase and THF (in parentheses) of H_2SiLiF (**R**) reactions with HCl, H_2S, PH_3, and SiH_4.

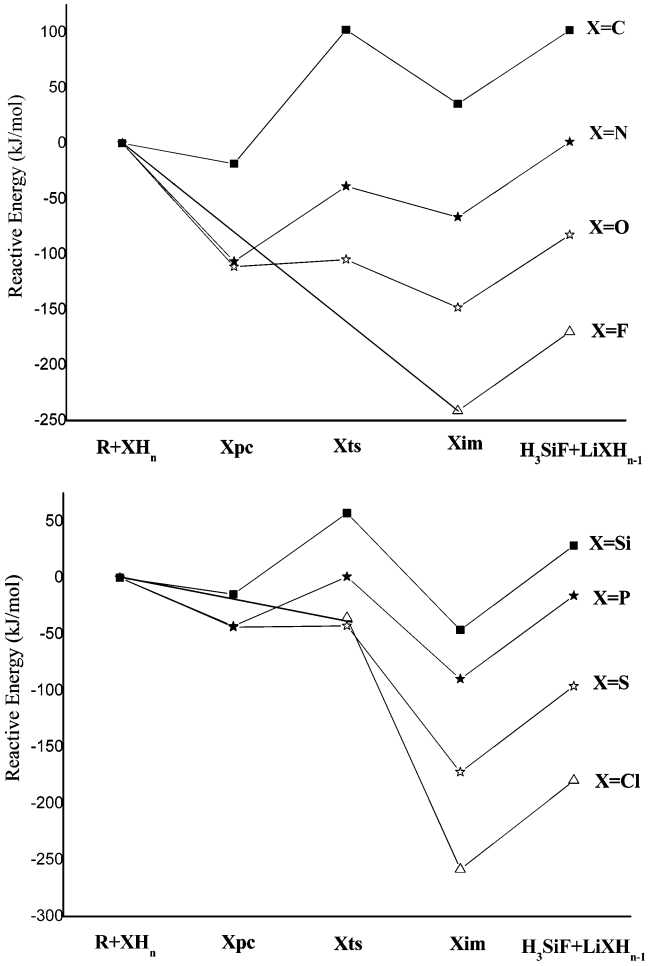

Figure 4. Potential energy surface profiles along the reaction pathways of **R** + XH_n in the gas phase at the B3LYP/6-31G(d,p) level.

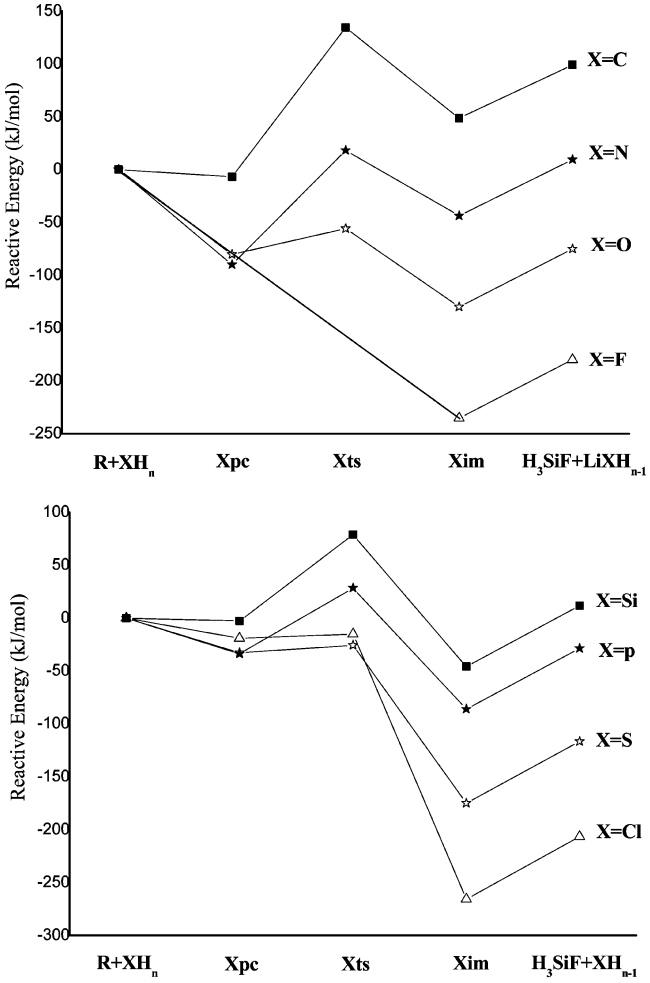

Figure 5. Potential energy surface profiles along the reaction pathways of **R** + XH_n in THF solvent at the B3LYP/6-31G(d,p) level.

row in the periodic table. The reactions of the second-row hydrides have lower barriers (from precursor complex to transition state) and are more exothermic than those of the first-row hydrides. That is, the reactions of the second-row hydrides proceed more easily than those of the first-row hydrides. Since the substitution reactions involve the breaking of X−H bonds, their strength becomes an important role. It is well-known that the X−H bond strength for the first-row hydride is bigger than that for the corresponding second-row hydride. Namely, the O−H bond in the H_2O molecule is more difficult to break than the S−H bond in H_2S. Therefore, the activation barrier of the H_2S (43.7 kJ/mol) reaction is lower than that of the H_2O (67.7 kJ/mol) reaction.

3.3. Solvent Effects of Reactions of H_2SiLiF (R) with XH_n. The experimental studies of silylenoids are usually carried out in solvents, and tetrahydrofuran (THF) is the most common solvent,[2] so the solvent effects in THF are also considered. In order to compare with the reaction results in the gas phase, the geometries of all structures obtained in THF solvent are also given in Figures 1 and 3 (in parentheses). The relative energies (relative to the corresponding reactants) in the THF solvent are given in Table 3.

The calculational results show that the reaction mechanism of **R** with XH_n in THF solvent is the same as that in the gas phase. As shown in Figures 1 and 3, the Si−Li distances in **R** and **Xpc** in THF solvent are about 0.2 Å longer than those in the gas phase, respectively. It is well-established that the polar solvents favor the more polar conformation. The positive Li atom is apart from Si atom making the dipole moments increasing. Therefore, **R** and **Xpc** are more stable in THF solvent than those in the gas phase, respectively. The geometries of other structures in THF solvent do not differ much from those in the gas phase. On the other hand, the total electronic energies of all structures in THF solvent are lower than those in the gas phase, respectively. Therefore, the presence of THF solvent makes the structures stable. The relative energies of all structures along the reaction pathways of **R** + XH_n are shown in Figure 5. It can be found from comparison between Figures 4 and 5 that the relative energies of **Xpc** and **Xts** are little higher in THF solvent than those in the gas phase, and the relative energies of **Xim** and products in THF solvent are similar to those in the gas phase. However, the relative energy order in THF solvent is the same as that in the gas phase. Therefore, the presence of THF solvent disfavors slightly the substitution reaction.

3.4. Comparison with Insertion and H_2-Elimination Pathways of R + XH_n. To obtain a better understanding of the reactivity of silylenoid H_2SiLiF, a comparison is made among the substitution, insertion,[4a] and H_2-elimination[4b] pathways of **R** + XH_n. To elucidate the results more distinctly, the representative **R** + H_2O system is discussed in detail, and the general rules are presented finally. The potential energy surface profiles along three reaction pathways of **R** + H_2O at the B3LYP/6-31G(d,p) level are collected in Figure 6. Several interesting results may be found in this figure. Qualitatively, it seems to be generally accepted that the substitution pathway is more favorable than the other pathways. The H_2-elimination

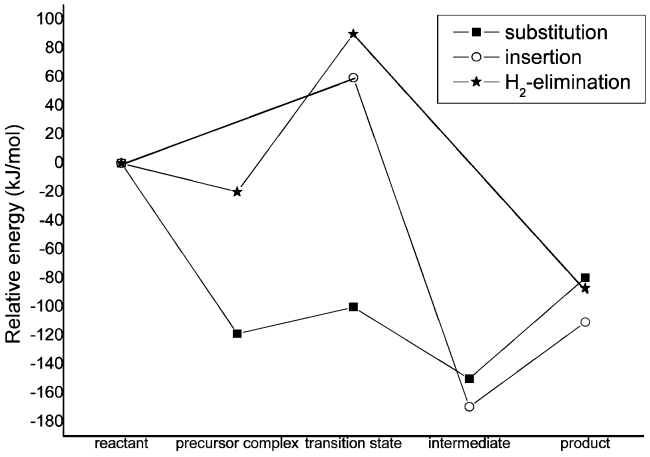

Figure 6. Potential energy surface profiles along three reaction pathways of **R** + H_2O at the B3LYP/6-31G(d,p) level.

reaction has the highest activation barrier and relatively small exothermicity.

As shown in Figure 2, the main part of the HOMO of **R** is localized on Si atom, and the main LUMO is localized on Li atom. The three-membered ring would be a reactive center because each bond in the ring is "loose" and weak, and it is easy to be destroyed when attacked by nucleophiles or electrophiles. The attractive interaction between the HOMO of H_2O and the LUMO of **R** leads to the substitution reaction. Furthermore, the relatively weak attractive interaction between the HOMO of **R** and the LUMO of H_2O makes the insertion reaction take place. However, only part of the HOMO in **R** is localized on two H atoms. This suggests that the H_2Si moiety in **R** would be weak reactive in chemical reactions, just where the H_2-elimination reaction takes place. Therefore, the H_2-elimination pathway should be unfavorable with higher barrier and lower exothermicity. As a whole, our theoretical results for the periodic trends of three reaction pathways are quite similar.

Considering the long-range interactions presented in Scheme 1, we have recalculated three pathways of the **R** + H_2O system at the MP2/6-31G(d,p) level. The MP2/6-31G(d,p) results suggest the same order of three reaction pathways as that of the B3LYP/6-31G(d,p) results. Changes of energies would not affect our conclusions qualitatively.

4. Concluding Remarks

In the present work, we have studied the substitution reactions of the three-membered-ring structure **R** of silylenoid H_2SiLiF with the first- and second-row XH_n molecules at the B3LYP/6-31G(d,p) level. The theoretical results suggest that a substitution reaction proceeds in a concerted manner via a five-membered-ring transition state to form the substituted product H_3SiF and $LiXH_{n-1}$.

There is a very clear trend toward lower activation barriers and more exothermic interactions on going from left to right along a given row in the periodic table. For the second-row hydrides, the substitution reactions are more exothermic than for the first-row hydrides and the reaction barriers are lower.

The presence of THF solvent makes the structures stable. However, the presence of THF solvent disfavors slightly the substitution reaction.

Compared to the previously reported insertions and H_2-elimination reactions of H_2SiLiF and XH_n, the substitution reaction pathway should be most favorable.

Acknowledgment. This work was supported financially by the National Nature science Foundation of China (No. 20373034), PhD Special Research Foundation of Chinese Education Department, the Project Sponsored by the Scientific Research Foundation of Yangzhou University, and High Performance Computational Center of Shandong University.

Supporting Information Available: Tables of total and relative energies of various structures in the gas phase and in THF solvent at theB3LYP/6-31G(d,p) level. This material is available free of charge via the Internet at http://pubs.acs.org.

References and Notes

(1) (a) Gilman, H.; Peterson, D. J. *J. Am. Chem. Soc.* **1965**, *87*, 2389. (b) Nefedow, O. M.; Manakow, M. N. *Angew. Chem.* **1964**, *76*, 270. (c) Miller, R. D.; Michl, J. *Chem. Rev.* **1989**, *89*, 1359. (d) Tamao, K.; Asahara, M.; Saeki, T.; Toshimitsu, A. *J. Organomet. Chem.* **2000**, *600*, 118.

(2) For experimental studies on silylenoids, see: (a) Wiberg, N.; Niedermayer, W. *J. Organomet. Chem.* **2001**, *628*, 57. (b) Boudjouk, P.; Samaraweera, U. *Angew. Chem., Int. Ed. Engl.* **1988**, *27*, 1355. (c) Tamao, K.; Kawachi, A. *Angew. Chem., Int. Ed. Engl.* **1995**, *34*, 818. (d) Tamao, K.; Kawachi, A. *Pure Appl. Chem.* 1999, 71.393. (e) Tamao, K.; Kawachi, A. *Organometallics* **1995**, *14*, 3108. (f) Sekiguchi, A.; Lee, V. Y.; Nanjo, M. *Coord. Chem. Rev.* **2000**, *210*, 11. (g) Lee, M. E.; Cho, H. M.; Lim,Y. M.; et al. *Chem. Eur. J.* **2004**, *10*, 377. (h) Likhar, P. R.; Zirngast, M.; Baumgartner, J.; Marschner, C. *Chem. Commun.* **2004**, 1764. (i) Kawachi, A.; Oishi, Y.; Kataoka, T.; Tamao, K. *Organometallics* **2004**, *23*, 2949. (j) Molev, G.; Bravo-Zhivotovakii, D.; Karni, M.; Tumanskii, B.; Botoshansky, M.; Apeloig, Y. *J. Am. Chem. Soc.* **2006**, *128*, 2784. (k) Lim, Y. M.; Cho, H. M.; Lee, M. E.; Baeck, K. K. *Organometallics* **2006**, *25*, 4960. (l) Harloff, J.; Popowski, E.; Reinke, H. *J. Organomet. Chem.* **2007**, *692*, 1421.

(3) For theoretical studies on silylenoids, see: (a) Clark, T.; Schleyer, P. R. *J. Organomet. Chem.* **1980**, *191*, 347. (b) Tanaka, Y.; Kawachi, A.; Hada, M.; Nakatsuji, H.; Tamao, K. *Organometallics* **1998**, *17*, 4573. (c) Feng, S. Y.; Zhou, Y. F.; Feng, D. C. *J. Phys. Chem. A* **2003**, *107*, 4116. (d) Feng, D. C.; Xie, J.; Feng, S. Y. *Chem. Phys. Lett.* **2004**, *396*, 245. (e) Feng, S. Y.; Lai, G. Q.; Zhou, Y. F.; Feng, D. C. *Chem. Phys. Lett.* **2005**, *415*, 327. (f) Flock, M.; Marschner, C. *Chem. Eur. J.* **2005**, *11*, 4635.

(4) (a) Xie, J.; Feng, D. C.; Feng, S. Y.; Zhang, J. *J. Mol. Struct. (THEOCHEM)* **2005**, *755*, 55. (b) Xie, J.; Feng, D. C.; Feng, S. Y. *Struct. Chem.* **2006**, *17*, 63.

(5) (a) Raghavachari, R.; Chandrasekhar, J.; Gordon, M. S.; Dykema, K. J. *J. Am. Chem. Soc.* **1984**, *106*, 5853. (b) Gordon, M. S.; Gano, D. R. *J. Am. Chem. Soc.* **1984**, *106*, 5421. (c) Heaven, M. W.; Metha, G. F.; Buntine, M. A. *J. Phys. Chem. A* **2001**, *105*, 1185.

(6) Frisch, M. J.; et al. *Gaussian 03*, revision B.01; Gaussian, Inc.: Pittsburgh PA, 2003.

(7) (a) Beck, A. D. *J. Chem. Phys.* **1993**, *98*, 5648. (b) Beck, A. D. *Phys. Rev. A* **1988**, *38*, 3098. (c) Vosko, S. H.; Wilk, L.; Nusair, M. *Can. J. Phys.* **1980**, *58*, 1200. (d) Lee, C.; Yang, W.; Parr, R.G. *Phys. Rev. B* **1988**, *37*, 785.

(8) (a) Gonzalez, C.; Schlegel, H. B. *J. Chem. Phys.* **1989**, *90*, 2154. (b) Gonzalez, C.; Schlegel, H. B. *J. Phys. Chem.* **1990**, *94*, 5523.

(9) (a) Miertus, S.; Tomasi, *J. Chem. Phys.* **1982**, *65*, 239. (b) Tomasi, J.; Persico, M. *Chem. Rev.* **1994**, *94*, 2027. (c) Cammi, R.; Tomasi, *J. Comput. Chem.* **1995**, *16*, 1449.

(10) Glendening, E. D.; Reed, A. E.; Carpenter, J. E.; Weinhold, F. NBO Version 3.1.